HIGH LIFT WAKE INVESTIGATION PROGRESS REPORT

The following was presented to the 13th AIAA Applied Aerodynamics Conference in June of 1995 as paper no. AIAA-95-1912, "Wake Measurements in a Strong Adverse Pressure Gradient", by J. P. Sullivan, S. P. Schneider, and R. Hoffenberg. It provides a reasonable summary of the experimental work being conducted.

Abstract

The behavior of wakes in adverse pressure gradients is critical to the performance of high-lift systems for transport aircraft. Wake deceleration is known to lead to sudden thickening and the onset of reversed flow; this 'wake bursting' phenomenon can occur while surface flows remain attached. Although known to be important for high-lift systems, few studies of such decelerated wakes exist. In this study, the wake of a flat plate has been subjected to an adverse pressure gradient in a two-dimensional diffuser, whose panels were forced to remain attached by use of slot blowing. Pitot probe surveys, L. D. V. measurements, and flow visualization have been used to investigate the physics of this decelerated wake, through the onset of reversed flow.

Introduction/Literature Review

The performance of an aircraft is strongly affected by the performance of its high-lift system. An example of a 150 passenger transport aircraft given in reference [7] shows that a 5% increase in takeoff lift/drag ratio results in a 15% increase in payload or an 11% increase in range. Also a 5% increase in maximum lift at landing gives a 20% increase in payload or a 3 knot decrease in approach speed for a significant reduction in landing length. Since vehicle cost, weight, and serviceability are influenced by the high-lift system, performance improvements must result from advancements in aerodynamics, not increased system complexity.

Some of the difficulties associated with high-lift aerodynamics are apparent in figure 1, which includes only two-dimensional effects.[7] Multi-element slotted airfoils such as this can have regions of interaction between upstream element wakes and boundary layers on downstream elements. If flow turning angles become significant, such 'confluent' boundary layers can be accompanied by strong adverse pressure gradients. When the low energy flow of a wake encounters the adverse gradient created by a downstream element, the wake decelerates and may even reverse. This type of off-the-surface flow reversal or 'bursting' is discussed in reference [13], and is believed to be responsible for the 'reverse' Reynolds number effects described in reference [7]. Klausmeyer et al. also discuss reverse Reynolds number trends in reference [6]. This is one of several papers which speculate that wake deceleration limits high-lift performance.

In his well known review of high-lift aerodynamics, Smith provides a simple analysis using Bernoulli's equation to show that wake reversal is possible, citing an analysis due to Gartshore.[4,13] Smith points out that according to Gartshore's analysis, boundary-layer separation is more likely to occur than 'off-the-surface' separation. He concludes that more study of this phenomenon is desirable. Wake reversal does appear to have been captured in a study by Braden et al., who measured the flow field around a GAW-1 multi-element airfoil, though the authors do not discuss the issue.[2] A few other studies, outlined in reference [12], have noted the presence of wake bursting, but none of these have examined it specifically.

Some observations of wake reversal were published by Petrov.[9] In this experiment, a tufted rectangular wing was tested using endplates, with various configurations of leading and trailing edge devices. Tufts were also used in the free-stream, attached to rods mounted normal to the surface of the airfoil near mid-

span. For the two-slot flap, "*... it was found...that the reduction in the rate of lift gain* C_{L_α} *... is associated with the appearance of a region of flow reversal, situated at some distance from the wing surface a distance commensurable with the thickness of the air stream passing through slots in the flap. At the same time, the flow directly on the wing and flap surfaces does not separate. The flow reversal region ... becomes thicker with increasing flap angle and angle of attack.*"[9] At larger flap deflections, the flow over the flap separated. Off-the-surface 'separation' was observed to limit the maximum obtainable lift. The above observations made by Petrov emphasize the importance of wake deceleration in high-lift systems.

Systematic mean velocity measurements of a decelerated wake were performed by Hill et al., years before the high-lift application was recognized.[5] The wake of a rectangular bar was passed through a two-dimensional diffuser with suction slots, and studied at several stations with a 3-hole probe. When a transverse velocity profile was assumed, measured freestream velocities were compared to a momentum-integral approximation with acceptable results.

Besides this early work, there has been relatively little detailed research into wake deceleration, although it seems to have become generally accepted that it is an important high-lift problem. Some of the references cited above have observed rapid wake growth in the flow field around a high-lift system, but none have made detailed turbulence measurements, or used smoke flow visualization to investigate this particular phenomenon. If information of this type was available, it might lead to a turbulence model for wakes in adverse pressure gradients, or at least help to predict how the wake will grow and affect the potential flow field. It was concluded by Alber that "*When external pressure gradient effects from the outer inviscid flow become dominant...it is clear that the scaling for inner wake development will be noticeably altered.*"[1] Incorporating empirical information on wake behavior in adverse pressure gradients into high-lift design codes could significantly benefit the next generation of transport aircraft.

Experiment

Because of the interest in wake deceleration, it was decided to investigate this effect specifically, on a fundamental level. A simple 6 foot flat plate was used to generate a wake, and a variable angle diffuser was built behind it to create an adverse pressure gradient (see figures 2 - 4). The flat plate was mounted in a 12" x 18" open return subsonic wind tunnel, which for this study was operated at 25 ft/s (Re = 1 million). Since the boundary layers on the diffuser panels separated before the wake reversed, tangential blowing slots, driven with high pressure air, were incorporated into the moveable panels (see figure 3). Blowing kept the boundary layers attached at diffuser angles large enough to reverse the wake of the flat plate. The diffuser was terminated with a duct 4 feet in length, designed to provide an outflow boundary condition for future modeling efforts (see figure 4).

Pressure and L.D.V. velocity measurements were performed in this flow-field. For the pressure measurements, a Pitot-static probe, connected to a Validyne pressure transducer, was scanned with a stepper motor driven, computer controlled X-Z traverse. Pressure data were acquired with a 12 bit PC data acquisition board. A single component argon-ion forward scatter system was used to make the L.D.V. measurements. Since this system included a Bragg cell, it was free from the directional ambiguity associated with the Pitot probe. The L.D.V. was traversed automatically on a motorized platform (see figure 5). Three passes were made at each diffuser angle, one measuring velocity in the streamwise direction, and two scans at inclinations ± 45 degrees. Mean quantities for Reynolds shear stress and transverse turbulence were then determined from the following relations:

$$\overline{v'^2} = \overline{u'^2_{+45}} + \overline{u'^2_{-45}} - \overline{u'^2} \qquad \overline{u'v'} = \frac{1}{2}\left(\overline{u'^2_{+45}} - \overline{u'^2_{-45}}\right)$$

To gain further insight into the physics of the flow, nichrome wires were suspended at several locations in the diffuser. An electric current was passed through one of these wires to rapidly heat it. Dripping kerosene or propylene glycol down the wire before heating it would send a burst of smoke into the flow at a given location. A pulsed light sheet from a Lumonics Nd:YAG laser illuminated the flow, while a Sony XC-77RR video camera recorded the image. These images were digitized with an EPIX frame grabber board for further study.

Discussion

With no adverse gradient, the flow-field behind the plate formed an ordinary two-dimensional turbulent wake. In general, when viscous flow leaves a flat plate, the no-slip boundary condition is no longer present, and the boundary layers from the upper and lower plate surfaces (figure 6) merge to form a wake. This wake then slowly evolves over several chord lengths, as the effect of the wall shear stress disappearance diffuses outward.[3] Wakes such as this are typically divided into three regions. The first begins at the end of the flat plate, and may extend to 25 momentum thicknesses or so.[10] This near wake is where the laminar sublayer of the upstream boundary layer is destroyed. The second, or intermediate region, consumes the logarithmic region of the plate's boundary layer. The far wake begins about 350 momentum thicknesses downstream of the trailing edge, when the mixing is complete. At this point asymptotic power laws are valid, although self-similar behavior is sometimes observed sooner.[10]

I. Zero Pressure Gradient

With the diffuser angle set to zero degrees, the wake was not exposed to any external pressure gradient, permitting comparison to other published measurements in flat plate wakes. L.D.V. mean velocity profiles agreed well with Pitot probe measurements (see figure 7), and turbulence data corresponded to traditional flat plate wake profiles (see figures 8-9).[3,11]

II. Moderate Adverse Pressure Gradient

In this investigation, measurements were taken for several diffuser angles at stations in the near and intermediate wake, both of which have high-lift implications. At the diffuser angles used to create moderate pressure gradients, boundary layers adhered to the moveable diffuser panels reasonable well, so slot blowing was not used. L.D.V. surveys at the trailing edge of the flat plate fell within the domain of the near wake. Since the flow was just entering the diffuser, it was only exposed to the external pressure gradient for a very short distance. As a result, mean velocity and turbulence quantities were unaffected by diffuser angle (see figures 10-12). It should be noted that 'Uo' was chosen to be the freestream velocity at the entrance to the diffuser. Figure 11 also shows a high turbulence level directly behind the trailing edge of the flat plate. This seems rational, since it is there that two separate boundary layers are suddenly combined. This behavior was not present in surveys taken at the end of the diffuser. Because $x / \theta \approx 275$, this location was clearly in the intermediate wake. Unlike the near wake case, turbulence measurements at the end of the diffuser showed a relative minimum at the wake center, where the shear stress equals zero (see figures 13 & 14). Physically, this indicated how the wake had adjusted to the absence of the solid surface which separated the two boundary layers further upstream. The minor asymmetry in the turbulence plots is due to slight imperfections in the facility. When the diffuser was opened between 0 and 6 degrees (half angle), the velocity deficit in the center of the wake grew in magnitude and width, due to prolonged exposure to the adverse gradient (see figures 15 & 16). Scans in the spanwise direction indicated the flow was uniform in the central region of the diffuser (see figure 17). Also noted was the relative insensitivity of Reynolds shear stress to pressure gradient at the near and intermediate wake stations (see figures 18 & 19). This finding may be in contrast to one by Nakayama, who found that "*Reynolds stresses, particularly the shear stress, are strongly influenced by the streamline curvature and the pressure gradient.*"[8] In that experiment, curvature and pressure gradient effects were coupled when a plate was inclined to the freestream. It is possible that the effects observed there were due more to curvature than pressure.

It is clear from the L.D.V. measurements that increases in diffuser angle had a less dramatic effect as 6 degrees was approached, due to separation of the boundary layers from the diffuser panels. However, with the aid of diffuser blowing, boundary layer attachment was maintained at larger diffuser angles, making it possible to subject the wake to stronger adverse pressure gradients.

III. Strong Wake Reversal

Without the 4 ft. duct, a very strong adverse gradient could be established, so it was removed for the 'strong reversal' investigation. To make preliminary observations, smoke wires were used with a pulsed YAG light sheet directed up the tunnel centerline. In figure 20, smoke is seen to travel downstream from the 'smoke wire' everywhere but in the wake, where the smoke is carried upstream. Smoke wire photography carried out at different locations showed that the point of reversal onset was about 12 inches downstream of the trailing edge. L.D.V. measurements also confirmed the presence of significant wake reversal (see figure 21).
It should be noted that the 'strong reverse' case was also a three dimensional flow-field. Spanwise photography showed smoke being carried to and from the diffuser side walls in regions where reversed flow was present. Although the side walls have less effect on central flow in the vertical plane than the moveable panels, they too are subjected to an axial pressure gradient, and may require boundary layer control when future tests are conducted at higher Reynolds numbers.

Severe reversal like this is intriguing, and is a comparatively unexplored flow, but from an applied perspective the most interesting case may be that of reversal onset, since this is where maximum lift would most likely occur.

IV. Reversal Onset

With the rectangular duct back in position, L.D.V. measurements were taken for the case of reversal onset at three axial locations in the diffuser (see figure 22). With a diffuser half-angle of 14 degrees, and slot blowing to keep the boundary layers attached, smoke photography confirmed the presence of reversed flow at the diffuser exit. L.D.V. measurements taken at the same location showed no negative mean velocities, so clearly most of the turbulent wake was flowing in the forward direction for the reversal onset condition (see figure 23). The wake was clearly much broader than in the case of weaker pressure gradients, and transverse turbulence increased noticeably (see figures 24 & 25). Measurements taken at 3/4 of the diffuser length were similar to those at the exit, with some minor decreases in magnitudes and wake width (see figures 26-28). At the 1/2 station, the inviscid mean velocity profile appeared more uniform than was the case at the downstream locations mentioned above (see figure 29). Since the blowing slots were located just downstream of the 1/2 station, they had less influence on measurements performed there. Turbulence profiles taken at 1/2 the diffuser length showed reductions in wake growth consistent with results from the other two locations (see figures 30-31).

Conclusions

A turbulent wake was decelerated to varying degrees and studied with L.D.V., pressure probes, and flow visualization. As the adversity of the imposed pressure gradient was increased, the wake became thicker and the turbulence level greater. Wake thickness more than tripled when it was taken from zero pressure gradient to the point of reversal onset. Wake growth of this sort would clearly affect the inviscid flow in a high lift system. The mean velocity and turbulence data presented here may now be incorporated into a turbulence model, perhaps as a module in a more general code. The next generation of high-lift systems will be designed with such tools, that reflect an improved understanding of this phenomenon so important to their aerodynamics.

Computational Simulation

Since the preceeding experimental work was presented, an attempt has been made to simulate the flow-field with INS-2D, a two-dimensional Navier-Stokes code. HYPGEN, a hyperbollic grid generator, was used to create grids such as those shown in figure 32. The evolution of streamwise mean and turbulent velocity in the absence of a pressure gradient is plotted in figures 33 & 34. Comparisons with experimental data are encouraging (see figures 35 & 36), though clearly some turbulence models will better simulate this flow than others. While simpler models such as Baldwin-Barth and Spalart-Allmaras are reasonably effective in predicting the magnitudes of mean turbulence quantities, the two-equation k-omega model is better suited to determing the shape of turbulence profiles. It is not yet known how these models will behave in stronger adverse pressure gradients, such as those encountered in high-lift flow. Examining the strengths and weaknesses of several turbulence models in simulating this flow-field will assist in developing future models better suited to predicting the behavior of high-lift flows.

Acknowledgments

This research was supported by grant # NAG-2-854 from NASA Ames Research Center. Thanks are owed to Larry Erickson and Stuart Rogers for providing the resources, source code, and assistance which made the computer simulations possible.

References

1. Alber, I. E.. Turbulent Wake of a Thin, Flat Plate. AIAA Journal, 18(9):1044-1051, 1979.

2. Braden, J. A., Whipkey, R. R., Lilley, D. E., Jones, G. S., and Morgan, H. L.. Application of Laser-Velocimetry to the Study of the Flow Around a Two-dimensional Airfoil. Paper 86-505, AIAA, 1986. AIAA 24th Aerospace Sciences Meeting.

3. Chevray, R. and Kovasznay, L., Turbulence Measurements in the Wake of a Thin Flat Plate, *AIAA Journal*, 7(8):1641-1643, August, 1969.

4. Gartshore, I. S.. Predictions of the Blowing Required to Suppress Separation from High-Lift Aerofoils. Paper 70-872, AIAA, 1970. CASI/AIAA Meeting on the Prospects for Improvement in Efficiency of Flight.

5. Hill, P. G., Schaub, U. W., and Senoo, Y.. Turbulent Wakes in Pressure Gradients. *Journal of Applied Mechanics*, 30(12):518-524, December, 1963.

6. Klausmeyer, S. M., and Lin, J. C.. An Experimental Investigation of Skin Friction on a Multi-Element Airfoil. Paper 94-1870, AIAA, 1994. AIAA 12th Applied Aerodynamics Conference.

7. Mack, M. D. and McMasters, J. H.. High Reynolds Number Testing in Support of Transport Airplane Development. Paper 92-3982, AIAA, 1992. AIAA 17th Aerospace Ground Testing Conference.

8. Nakayama, A.. Curvature and Pressure-Gradient Effects on a Small-Defect Wake. *Journal of Fluid Mechanics*, 175:215-246, 1987.

9. Petrov, A. V.. Certain Types of Separated Flow Over Slotted Wings. *Fluid Mechanics - Soviet Research*, 7(5):80-89, September-October 1978.

10. Ramaprian, B. R., and Patel, V. C.. The Symmetric Turbulent Wake of a Flat Plate. *AIAA Journal*, 20(9):1228-1235, September, 1982.

11. Ramjee, V., and Neelakandan, D., Curvature Effects on the Wake of an Airfoil and Other Bodies, *Fluid Dynamics Research*, 6:1-13. 1990.

12. Schneider, S., Campbell, B., Bucci, G., and Sullivan, S.. An Experimental Simulation of Flap Flow on Multi-element Airfoils at High Reynolds Number. Paper 94-2613, AIAA, 1994. AIAA 18th Aerospace Ground Testing Conference.

13. Smith, A. M. O.. High-lift aerodynamics. *Journal of Aircraft*, 12(6):501-530, June 1975.

Figures

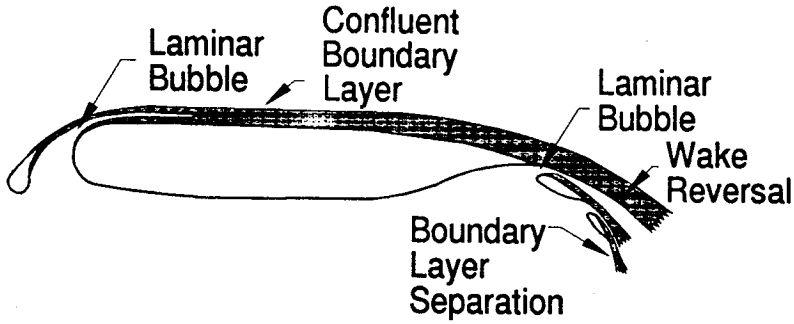

Figure 1. Flow over a Two-Dimensional High Lift Airfoil System.

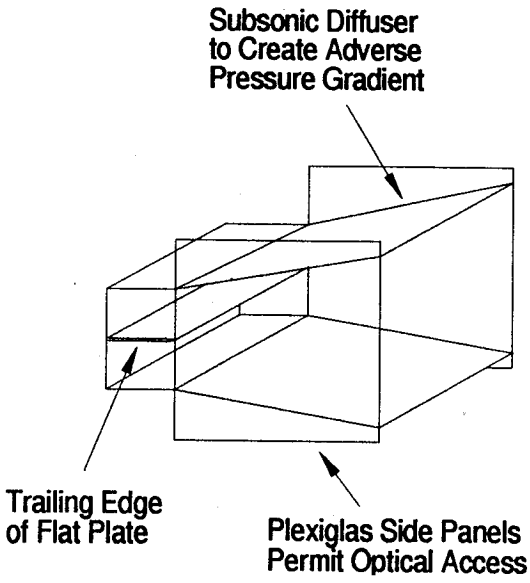

Figure 2. Diffuser Used to Create Adverse Pressure Gradient.

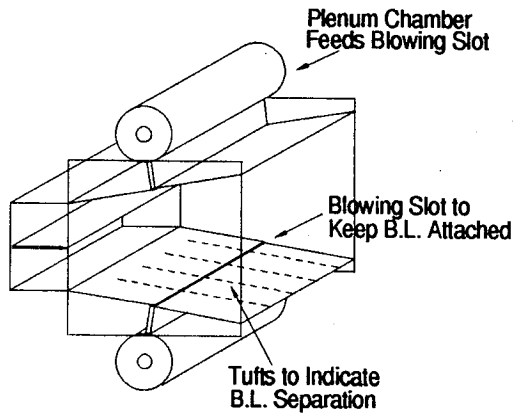

Figure 3. Diffuser with Active Boundary Layer Control Used to Produce 'Reversal Onset' and 'Strong Reversal'.

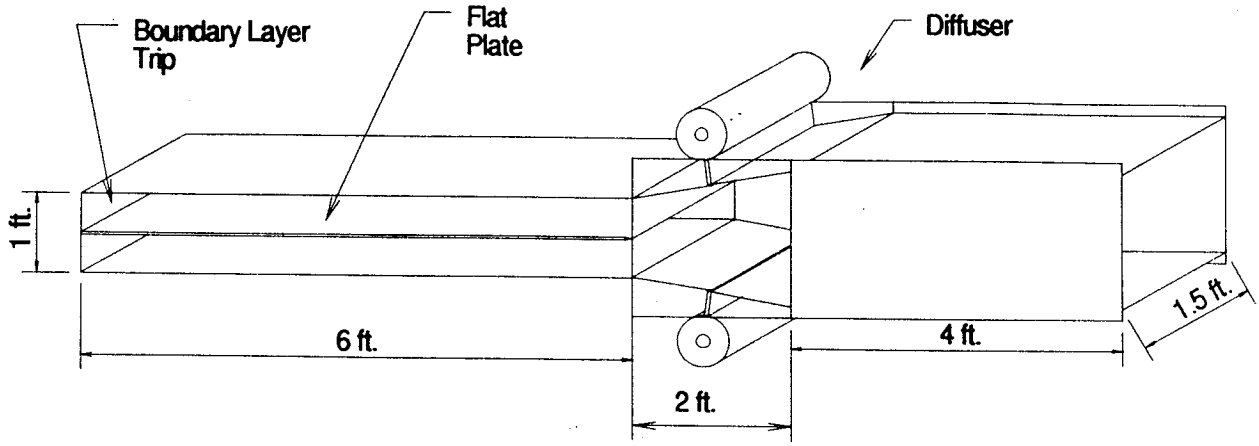

Figure 4. Layout of Facility.

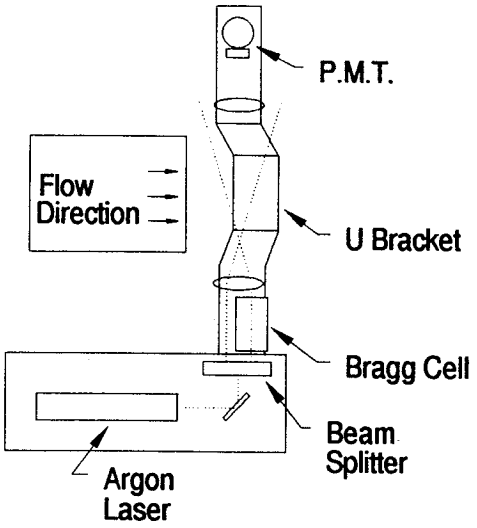

Figure 5. Top View of Forward Scatter L.D.V. System.

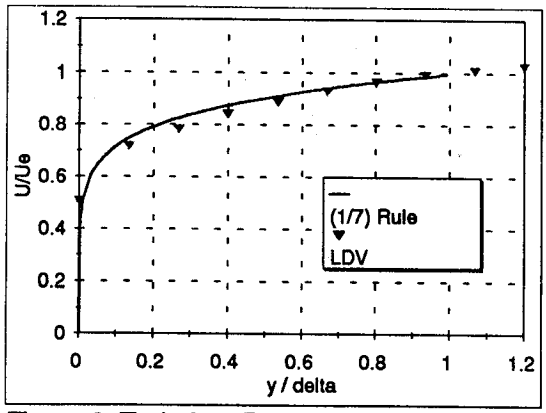

Figure 6. Turbulent Boundary Layer Profile on Flat Plate.

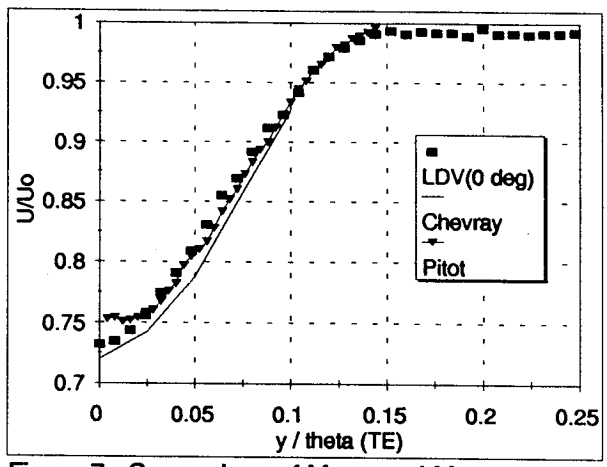

Figure 7. Comparison of Measured Mean Velocities at End of Diffuser.

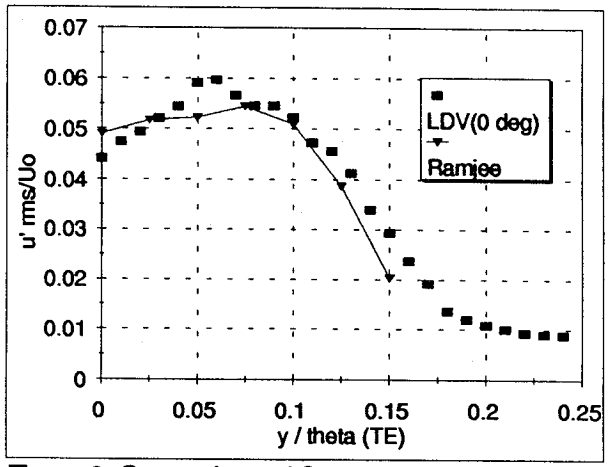

Figure 8. Comparison of Streamwise Turbulence Intensities at End of Diffuser.

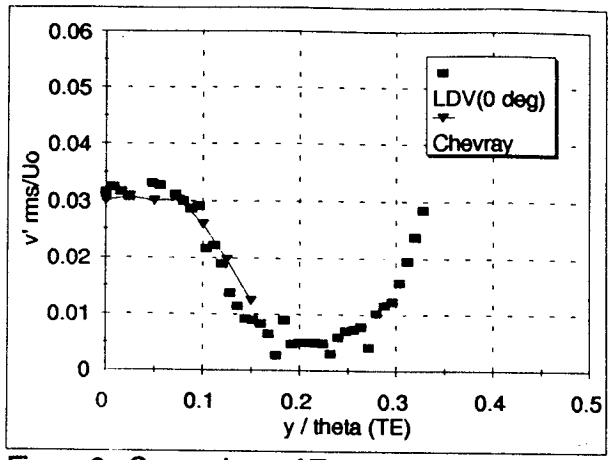

Figure 9. Comparison of Transverse Turbulence Intensities at End of Diffuser.

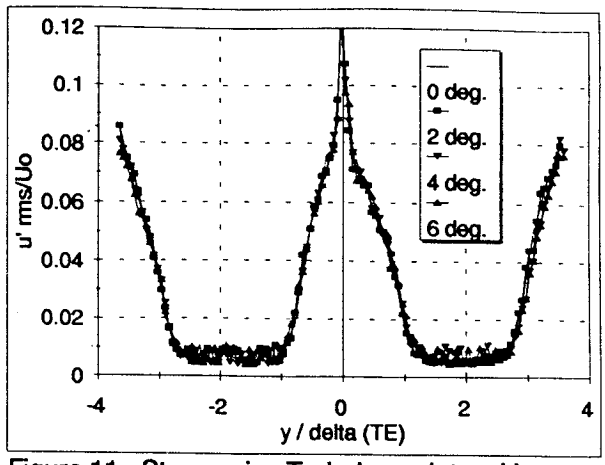

Figure 11. Streamwise Turbulence Intensities at End of Flat Plate.

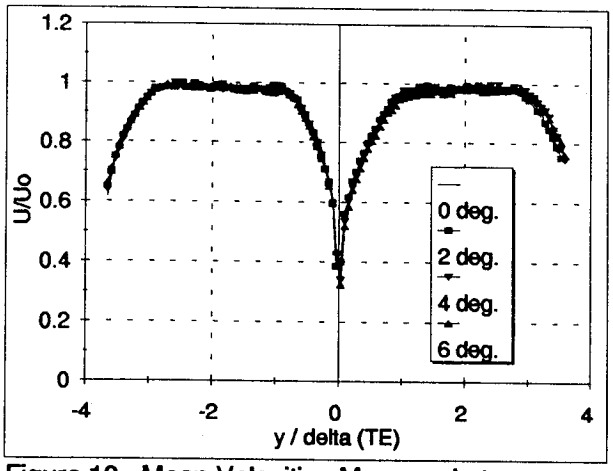

Figure 10. Mean Velocities Measured at End of Flat Plate for Several Diffuser Angles.

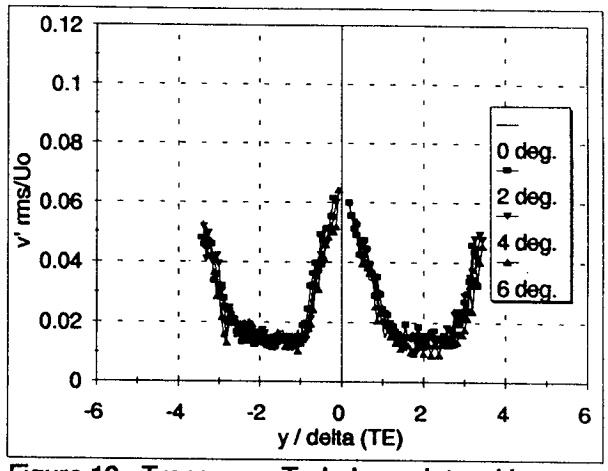

Figure 12. Transverse Turbulence Intensities at End of Flat Plate.

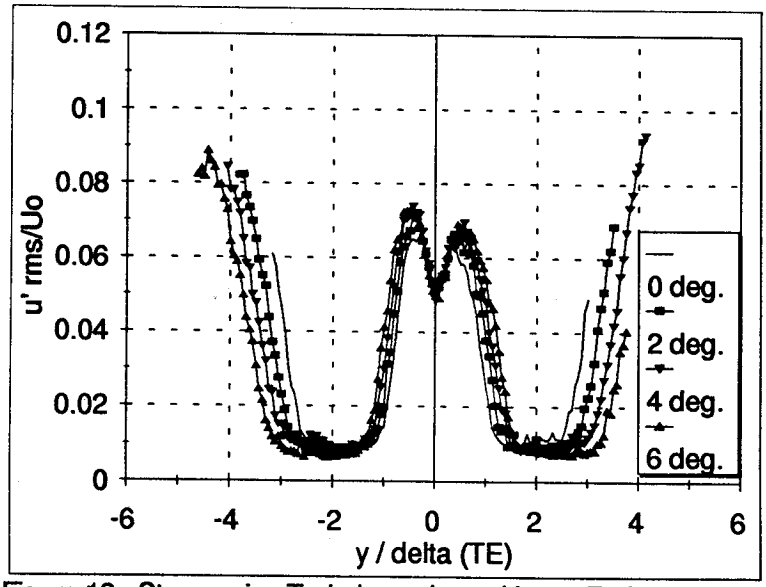

Figure 13. Streamwise Turbulence Intensities at End of Diffuser.

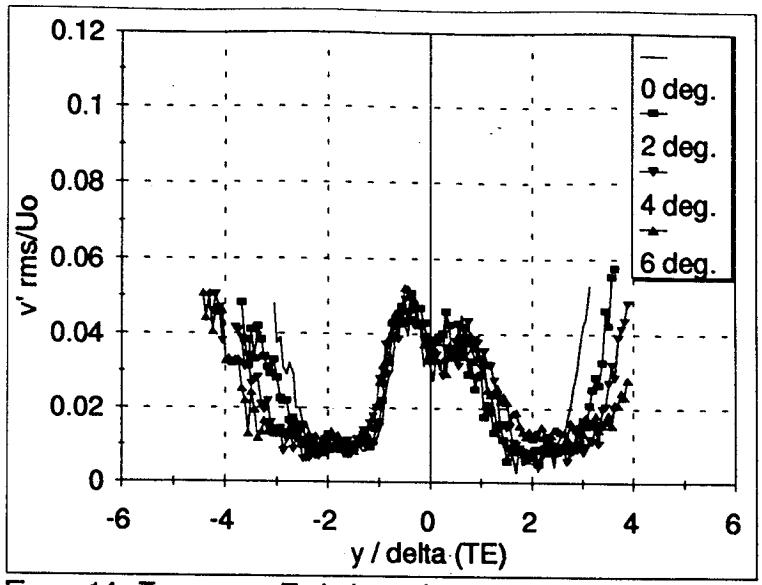

Figure 14. Transverse Turbulence Intensities at End of Diffuser.

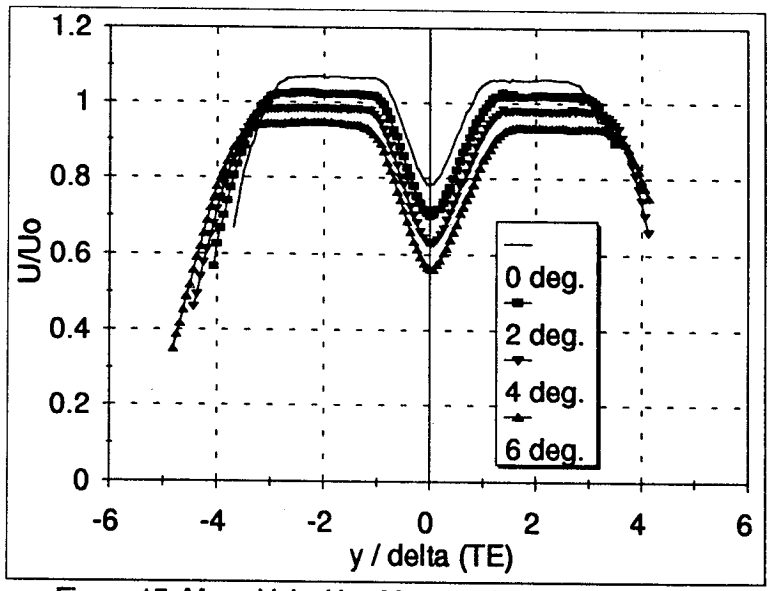

Figure 15. Mean Velocities Measured at End of Diffuser.

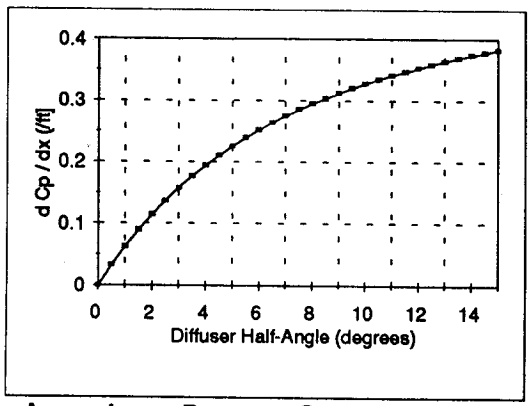

Figure 16. Approximate Pressure Gradient Created by Diffuser.

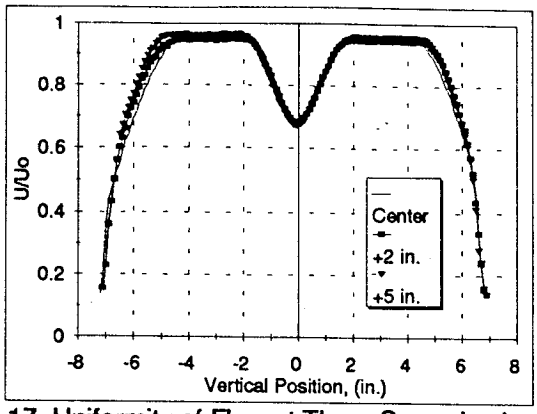

Figure 17. Uniformity of Flow at Three Spanwise Locations

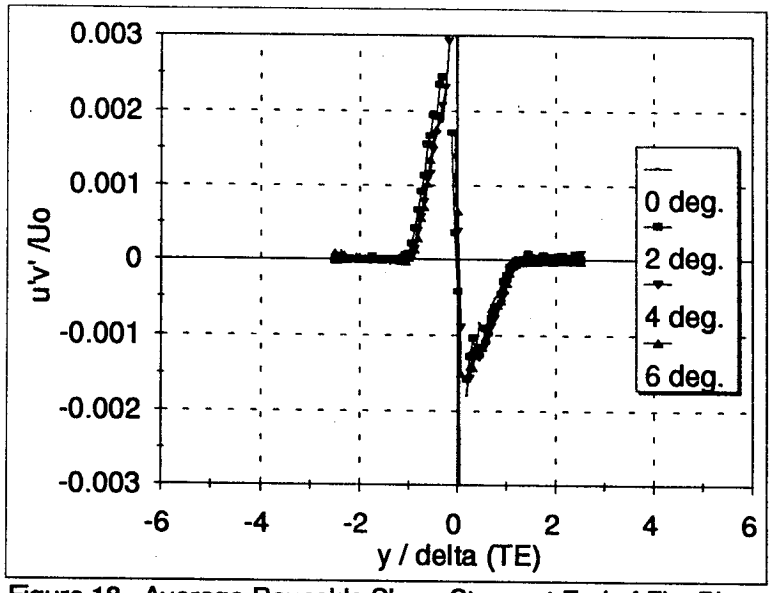

Figure 18. Average Reynolds Shear Stress at End of Flat Plate.

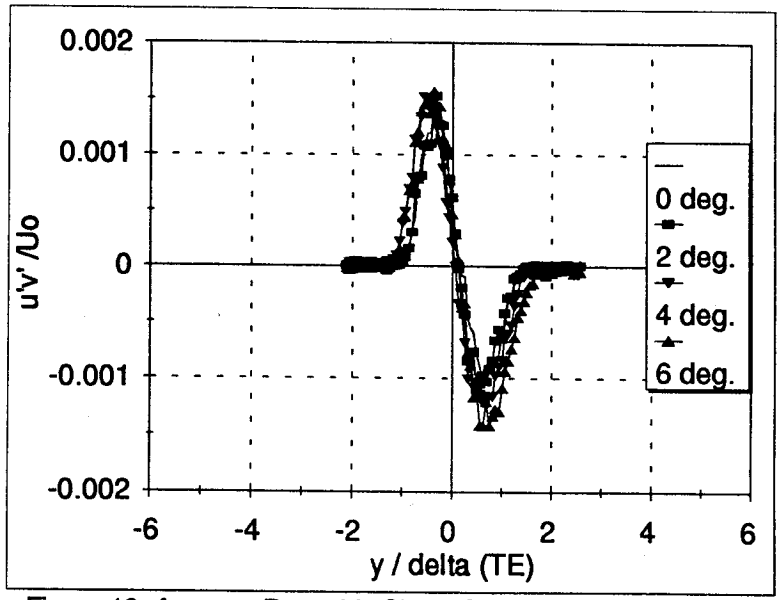

Figure 19. Average Reynolds Shear Stress at End of Diffuser.

Figure 20. Photograph of Reversed Wake Flow. Termination Duct Removed to Obtain Strong Reversal.

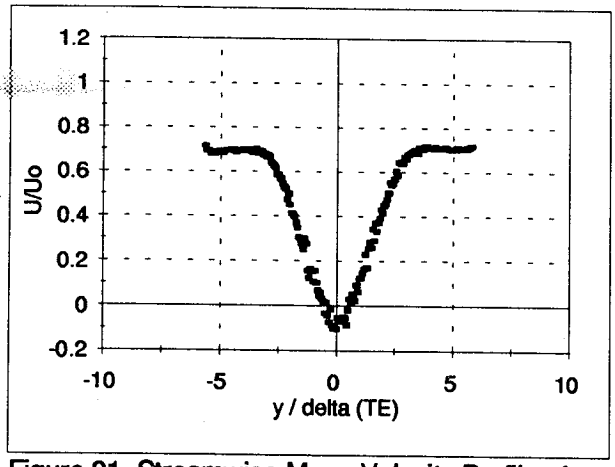

Figure 21. Streamwise Mean Velocity Profile of Strong Wake Reversal at End of Diffuser, Termination Duct Removed.

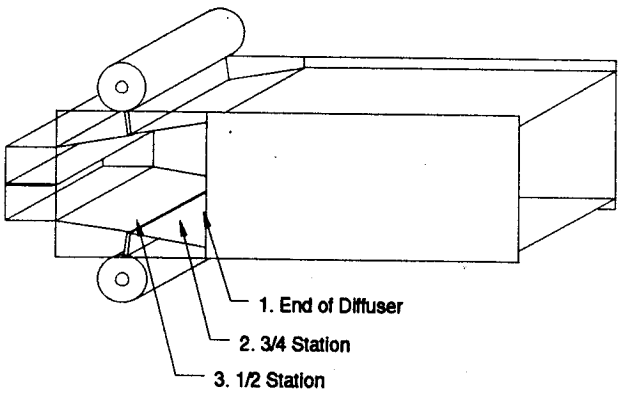

Figure 22. Survey Locations for Investigation of Reversal Onset.

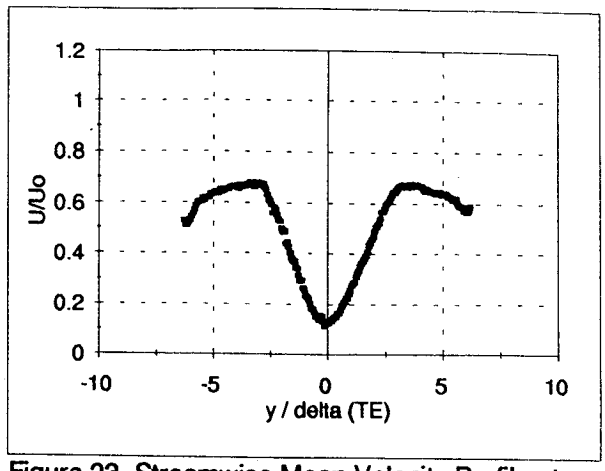

Figure 23. Streamwise Mean Velocity Profile at Reversal Onset, End of Diffuser.

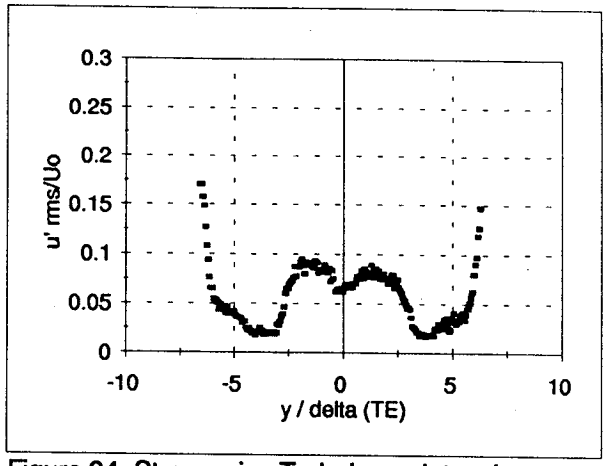

Figure 24. Streamwise Turbulence Intensity at Reversal Onset, End of Diffuser.

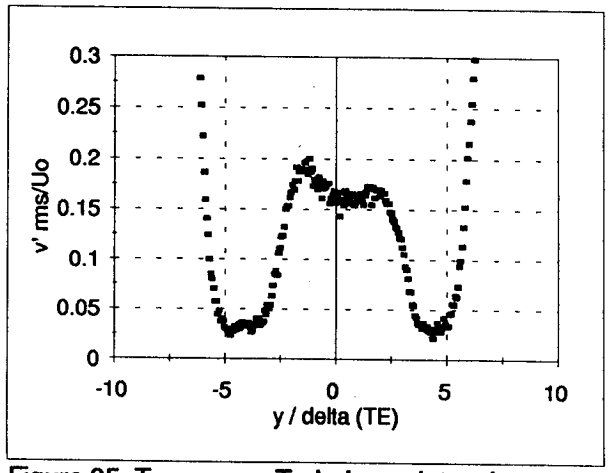

Figure 25. Transverse Turbulence Intensity at Reversal Onset, End of Diffuser.

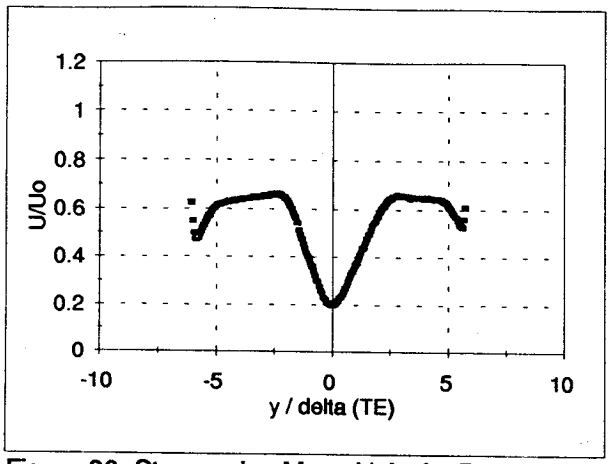

Figure 26. Streamwise Mean Velocity Profile of Reversal Onset at 3/4 Station.

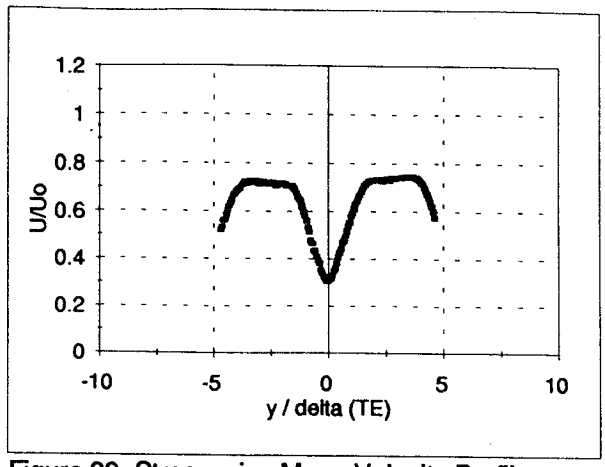

Figure 29. Streamwise Mean Velocity Profile at Reversal Onset at 1/2 Station.

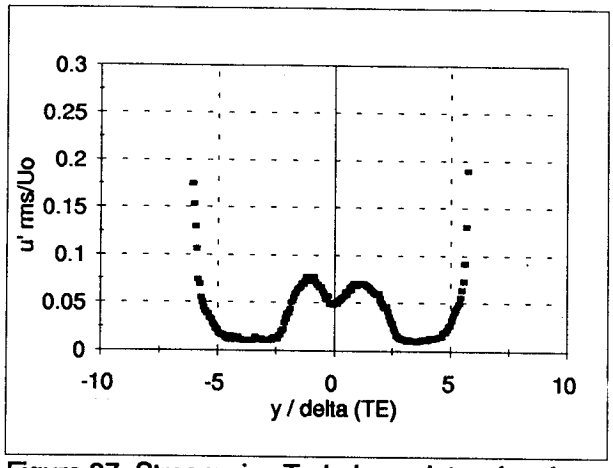

Figure 27. Streamwise Turbulence Intensity of Reversal Onset at 3/4 Station.

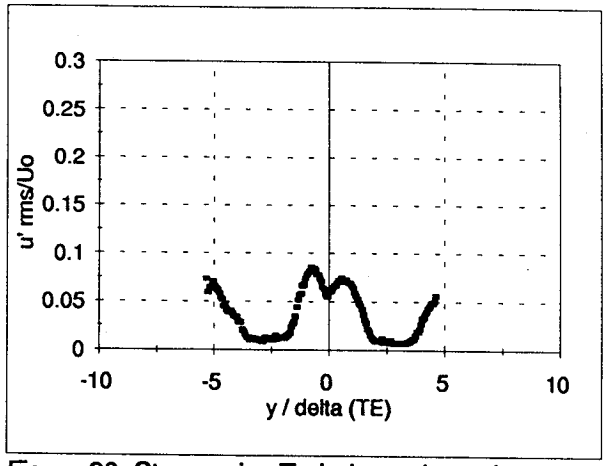

Figure 30. Streamwise Turbulence Intensity at Reversal Onset at 1/2 Station.

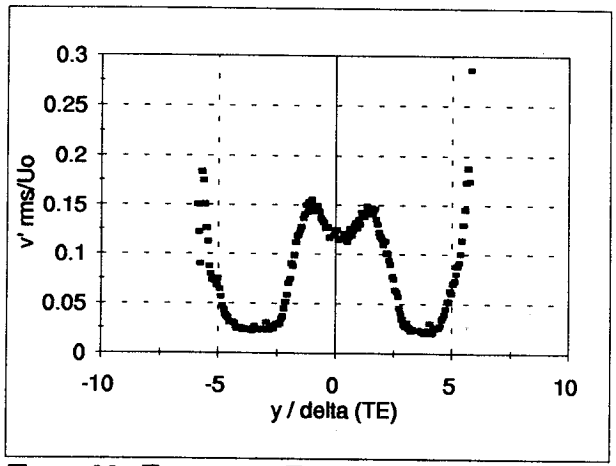

Figure 28. Transverse Turbulence Intensity of Reversal Onset at 3/4 Station.

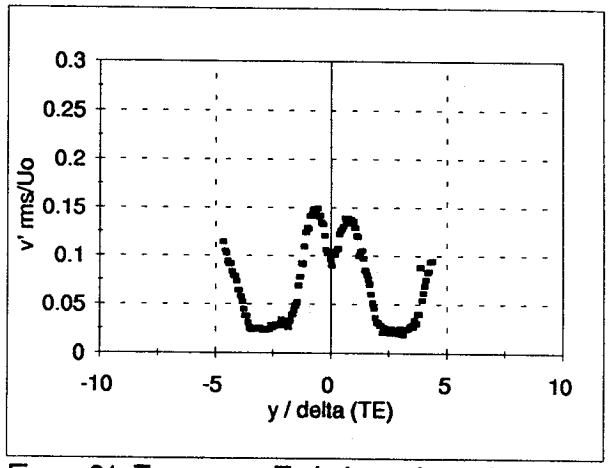

Figure 31. Transverse Turbulence Intensity at Reversal Onset at 1/2 Station.

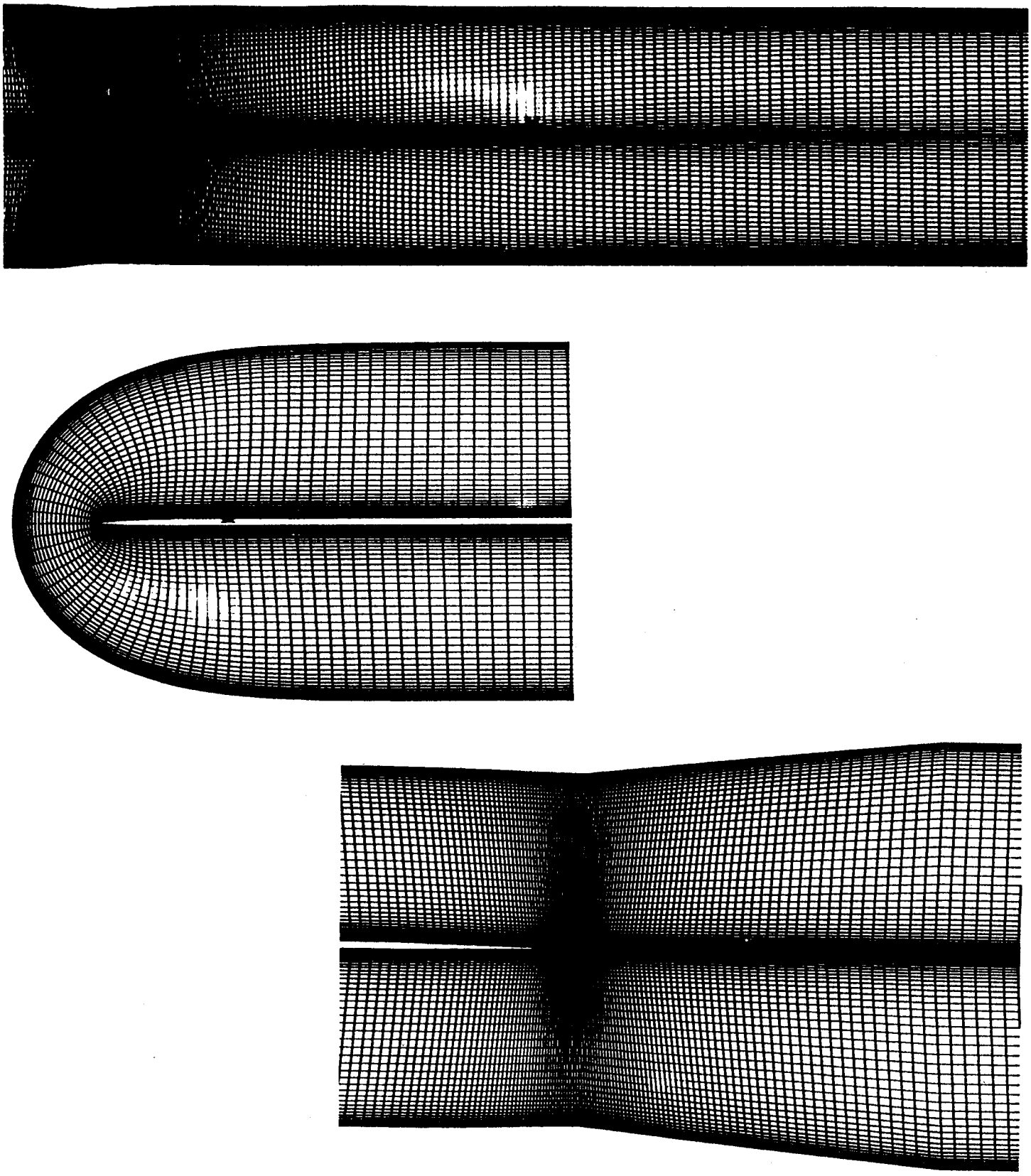

Figure 32. Computational Grids.

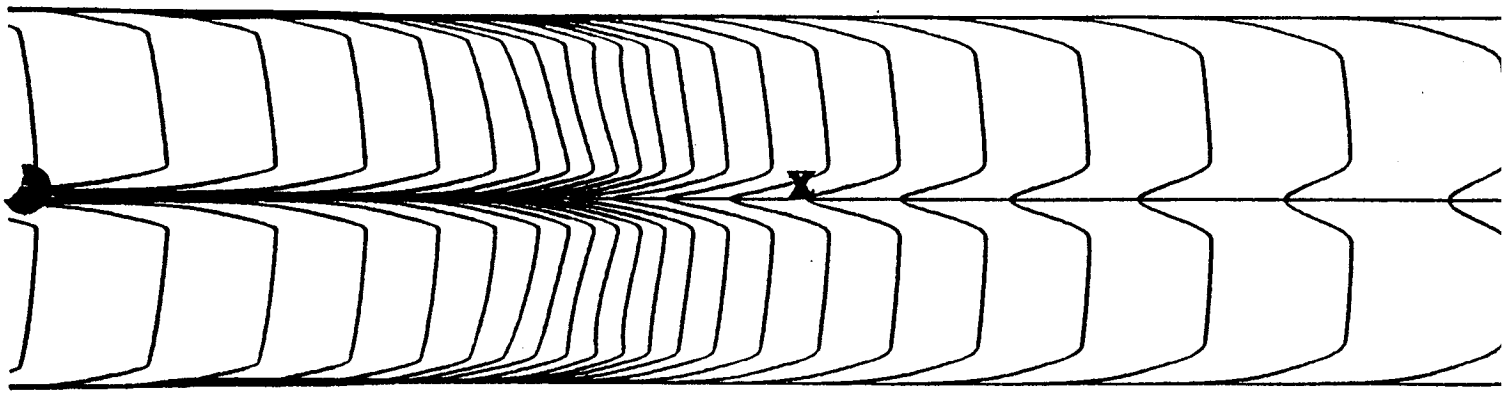

Figure 33. Development of Mean Velocity Profile, k-omega model.

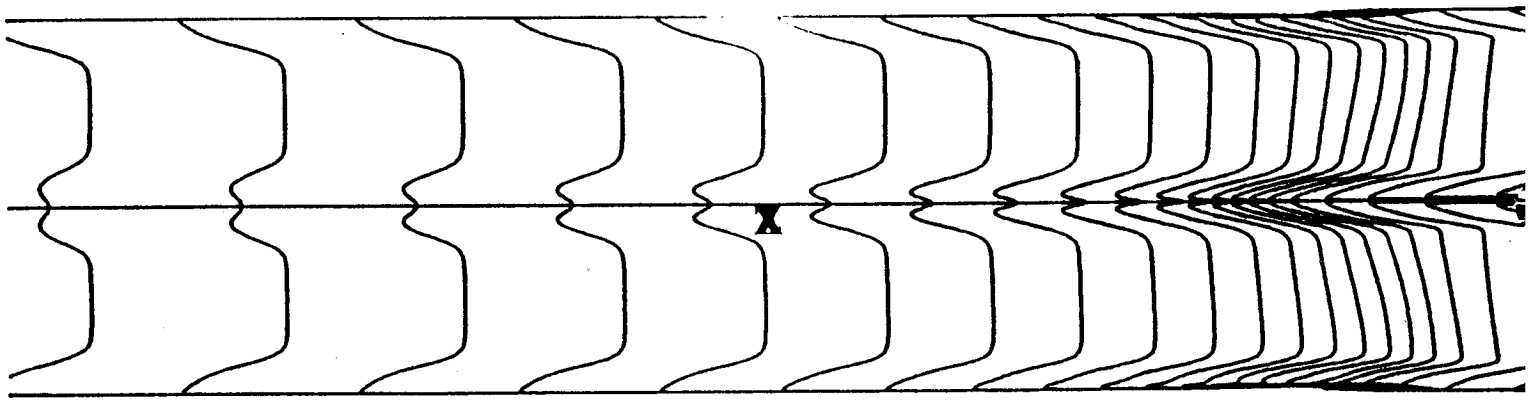

Figure 34. Development of Streamwise Turbulence Profile, k-omega model.

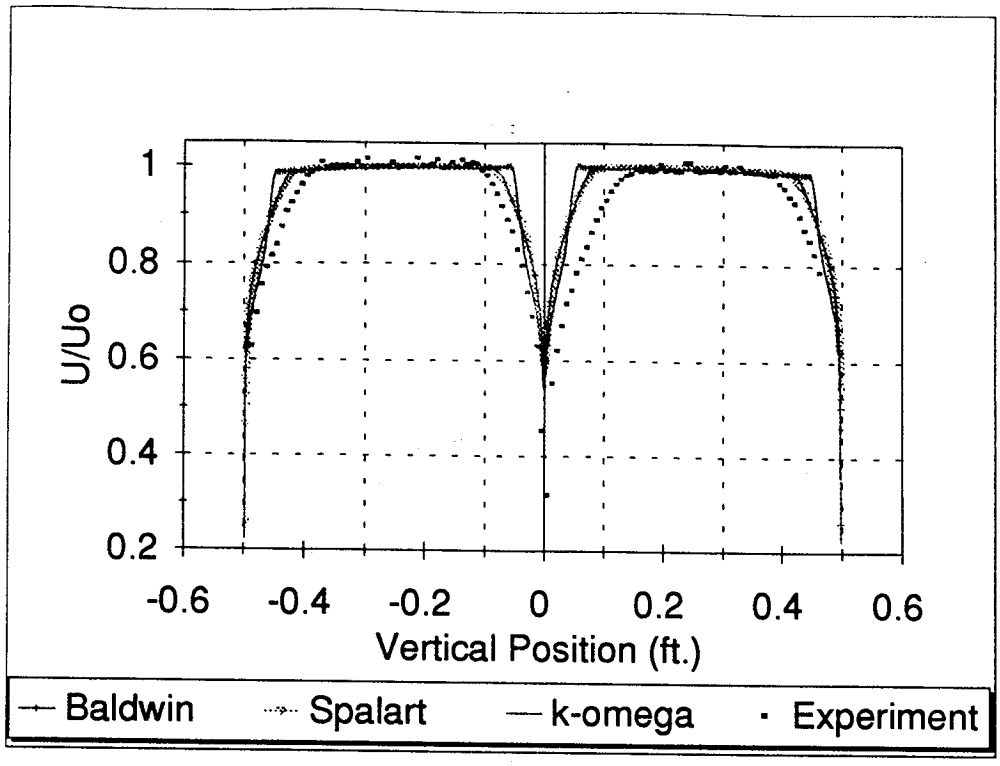

Figure 35. Comparison of Mean Velocities at End of Flat Plate.

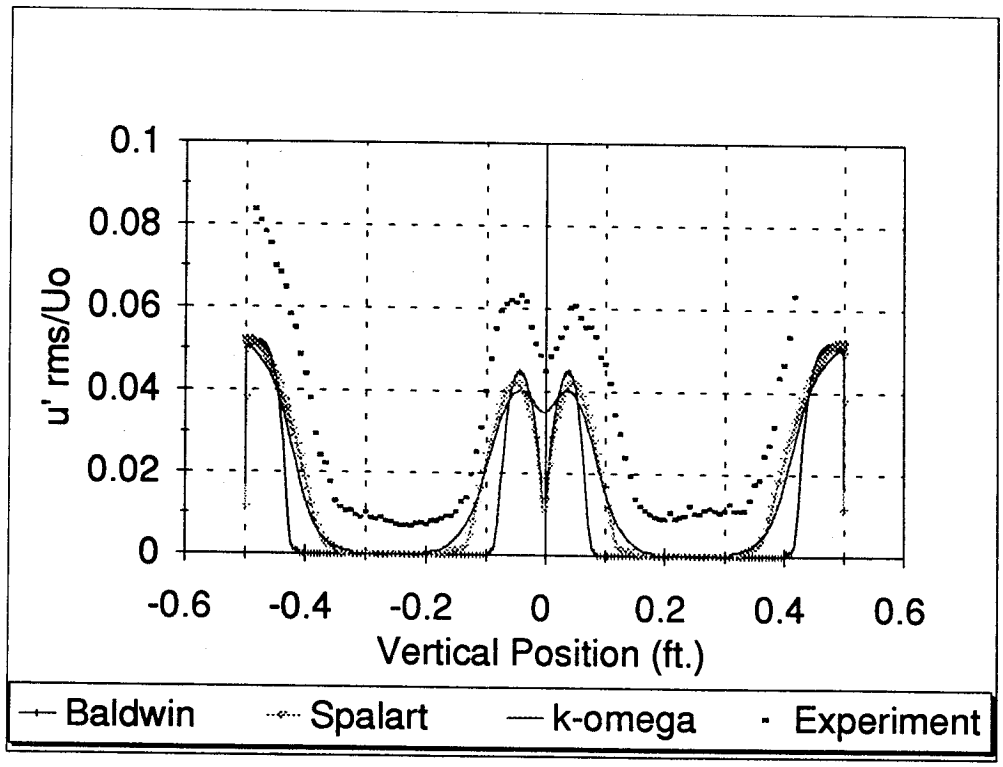

Figure 36. Comparison of Fluctuating Velocities at End of Diffuser.